Imaging-based Topographic Association and Dissociation between Tau Pathology and Atrophy Correlated with Impairments of Key Motor Domains in Progressive Supranuclear Palsy

Yuko Kataoka, MD, PhD,[1)] Kenji Tagai, MD, PhD,[1)] Ryoji Goto, MD, [1)] Kiwamu Matsuoka, MD, PhD,[1)] Kosei Hirata, MD, PhD,[1)] Keisuke Takahata, MD, PhD,[1)] Masaki Oya, MD,[1)] Hideki Matsumoto, DDS, PhD,[1)3)] Shin Kurose, MD,[1)] Masanori Ichihashi, MD,[1)] Sho Moriguchi, MD, PhD[1)], Hitoshi Shinotoh, MD, PhD,[1)] Naomi Kokubo, PhD,[1)] Yuki Momota, PhD, [1)] Chie Seki, PhD,[1)] Hitoshi Shimada, MD, PhD,[1)4)] Kazunori Kawamura, PhD,[2)] Ming-Rong Zhang, PhD,[2)] Takahiko Tokuda, MD, PhD,[1)] Makoto Higuchi, MD, PhD,[1)5)] Hironobu Endo, MD, PhD[1)]

[1] Advanced Neuroimaging Center, Institute for Quantum Medical Science, National Institutes for Quantum Science and Technology (QST), Chiba, Japan

[2] Department of Advanced Nuclear Medicine Sciences, Institute for Quantum Medical Science, QST, Chiba, Japan

[3] Department of Oral and Maxillofacial Radiology, Tokyo Dental College, Tokyo, Japan

[4] Department of Functional Neurology & Neurosurgery, Center for Integrated Human Brain Science, Brain Research Institute, Niigata University, Niigata, Japan

[5] Department of Neuroetiology and Diagnostic Science, Osaka Metropolitan University Graduate School of Medicine, Osaka, Japan

Correspondence to Hironobu Endo, M. D., Ph. D.
Advanced Neuroimaging Center, Institute for Quantum Medical Science, National Institutes for Quantum Science and Technology, Chiba 263-8555, Japan
E-mail: endo.hironobu@qst.go.jp
TEL: +81-43-251-2111

Running title: Association of Tau and Neurological Symptoms
Number of words in abstract: 244/250
Number of words in introduction: 500/500
Number of words in discussion: 1447/1500
Number of words in main text: 3590/4500
Number of figures: 3
Number of tables: 2
Funding: Disclosures and author roles are found in the online version of this article.

Abstract

[Objectives] This study aimed to compare the distributions of tau pathology and atrophy related to key motor symptom domains in progressive supranuclear palsy (PSP).
[Methods] Fifty-three PSP cases underwent neurological assessments, including the PSP Rating Scale, which covers six domains. Tau positron emission tomography with florzolotau (18F) and T1-weighted magnetic resonance imaging were acquired from these patients and 43 healthy controls to assess correlations of domain scores with tau accumulation and local brain volumes. Path analysis was performed to explore

spatiotemporal relationships between tau deposits and volume loss leading to individual domains.

[Results] Subcortical tau accumulation and atrophy showed significant spatial overlap and were closely associated with motor deficits. The "ocular motor" domain scores correlated with tau in the midbrain tegmentum and globus pallidus, and the "gait and midline" domain scores correlated with tau in the globus pallidus, thalamus, and subthalamic nucleus. In contrast, tau deposits and volume reductions in separate neocortical regions were linked to the manifestations. Indeed, the "limb motor" domain scores correlated with tau in the precentral and supplementary motor cortices and atrophy in the angular gyrus. Path analysis suggested that tau in subcortical structures may elicit local neuronal loss, impairing the "ocular motor" and "gait and midline" domains, while tau in the neocortex likely affects the "limb motor" domain through local and subsequent network-mediated neurotoxicity.

[Interpretation] High-contrast tau imaging clarifies the neuropathological basis of key symptoms in living PSP patients and highlights distinct tau-induced neurotoxic effects in subcortical versus neocortical regions.

Introduction

Progressive supranuclear palsy (PSP) is an idiopathic neurodegenerative disorder lacking effective treatments. Clinically, it manifests with motor impairments resembling Parkinson's disease, alongside distinctive features like ocular motor dysfunction and postural instability. Neuropathologically, PSP is characterized by

neuronal and glial inclusions composed of four-repeat tau isoforms, including globose tangles, coiled bodies, and tufted astrocytes. These tau aggregates predominantly affect subcortical structures such as the thalamus, subthalamic nucleus, and brainstem, although neocortical regions, particularly in the frontal lobe, are also frequently involved [1 2 3 4]. Accordingly, PSP is classified within frontotemporal lobar degeneration with tau pathology (FTLD-Tau) [5].

A hallmark of PSP in morphometric neuroimaging is midbrain atrophy, commonly recognized as the hummingbird sign[6], correlating with neurological deficits assessed by the PSP Rating Scale[7]. Tau deposits are thought to contribute to neuronal loss, particularly in the brainstem. However, the extent to which tau accumulation leads to regional volume loss through direct or network-mediated effects remains unclear. Investigating these processes in vivo could provide crucial insights into the pathological basis of symptomatic manifestations. While animal models expressing four-repeat tau isoforms exhibit neuronal loss[8], their ability to replicate PSP-specific neurotoxic mechanisms remains uncertain. Moreover, while PSP-derived tau fibril inoculation in rodents induces neuronal and glial tau pathologies[9], prominent neuronal death leading to measurable atrophy has not been observed.

Given these discrepancies, it is crucial to establish links among tau aggregation, neuronal loss, and functional decline using human data. Although postmortem studies have delineated tau inclusions in PSP brains[3, 10], they do not correlate with antemortem symptoms, underscoring the value of in vivo assessments to explore spatial relationships between tau pathology, brain atrophy, and symptom severity.

Recently, we developed a tau positron emission tomography (PET) radioligand, florzolotau (18F), which exhibits high contrast for various tau pathologies, including those in PSP[11]. florzolotau (18F) enabled in vivo visualization of tau deposits in the thalamus, subthalamic nucleus, basal ganglia, midbrain, and motor cortices in PSP patients[11, 12], findings align with neuropathological observations. Two independent studies have demonstrated a strong correlation between florzolotau (18F) retention in the subthalamic nucleus and/or midbrain and total PSP Rating Scale scores[11, 13]. Despite these results, large-scale PET investigations are warranted to elucidate the evolution of tau pathology and its impact on key clinical domains, such as impaired eye movements and gait abnormalities.

Previous studies using [^{18}F]flortaucipir examined tau pathology and brain atrophy in PSP patients across various symptomatic subtypes[14], but did not correlate imaging with motor deficits. Furthermore, an imaging-pathology correlation analysis suggested [^{18}F]flortaucipir has limited sensitivity for four-repeat tau aggregates in FTLD[15], questioning its utility for staging PSP[16].

This study aims to identify anatomical regions exhibiting tau deposition and/or volume decline in relation to disease progression and symptomatic deterioration in a mid-sized PSP cohort.

By examining the concordance and discordance between florzolotau (18F) PET and volumetric MRI, we seek to determine whether four-repeat tau accumulation induces neurotoxicity locally or via network-mediated pathways. Additionally, path analysis of cross-sectional data was implemented to estimate the chronological progression of tau-induced neuronal damage associated with symptom categories.

Methods

Participants

A clinical study was conducted at the National Institutes for Quantum Science and Technology, Japan, between January 2018 and June 2023. It involved 45 healthy controls (HCs) and 53 patients with progressive supranuclear palsy (PSP). The diagnosis of PSP was based on the International Parkinson and Movement Disorder Society clinical criteria[17].

HCs were defined as individuals aged 40 years or older with no history of neurological impairment, a Mini-Mental State Examination score of ≥28, a Montreal Cognitive Assessment score of ≥26, and a Geriatric Depression Scale score of ≤5 or no history of depression. They were recruited from our volunteer group. Aβ-positive cases were excluded based on visual assessment of ^{11}C-Pittsburgh Compound-B PET scans, independently reviewed by at least three experienced PET specialists [18]

PSP severity was assessed using the PSP Rating Scale [19], which includes the following domains: history, mentation, bulbar function, ocular motor function, gait and midline stability, and limb motor function.

MRI Studies

The participants underwent 3-T MAGNETOM Verio (Siemens Healthcare) and 3-T MAGNETOM Prisma (Siemens Healthcare) scanning. T1-weighted gradient-echo sequence imaging (sagittal orientation; 1-mm-thick sections; echo time [TE], 1.95 ms; repetition time [TR], 2,300 ms; flip angle, 9.0°; inversion time [TI], 900 ms; field of view [FOV], 250 mm; matrix dimension, 512 × 512 × 176) was executed for

coregistration of PET images into an individual anatomical space and their segmentation for region-based quantification.

PET Studies

Tau accumulation was assessed using PET with a radiophone florzolotau (18F) on a Biograph mCT Flow system (Siemens Healthcare; matrix dimension, 200 × 200 × 109; voxel size [mm], 2 × 2 × 2). List-mode event data were reconstructed into PET images using a filtered back-projection algorithm with a Hanning filter (6.0 mm full width at half maximum). The PET scan protocol in detail was provided elsewhere[11 20]. Each participant underwent a 20-min PET scan (frames: 4 × 5 or 2 × 10 min) 90 min after the intravenous injection of florzolotau (18F) (187.0 ± 8.7 MBq).

Data Analysis

Voxel-based analysis was conducted using tau PET images transformed into the standard brain space via

DARTEL (Details are provided in the eMethods section of the supplementary material.). Tau accumulation and brain atrophy in PSP versus HC subjects were analyzed by identifying clusters of voxels with a family-wise error (FWE) of $P < 0.05$ and the voxel number exceeding assigned values. The association of tau accumulation and brain volume with neurological symptoms was evaluated to pick up voxel clusters with predefined height and extent thresholds. P value of 0.01 was selected as a height threshold to explore all areas showing tau depositions correlated with symptoms, and P value of 0.001 was employed to identify core regions pivotally involved in the link between tau pathology and manifestation. Meanwhile, $P < 0.001$ was selected to search for primary locations with atrophy related to symptoms since the use of a P value of 0.01 highlighted excessively broad areas containing voxels without notable volume loss.

Based on voxel-wise analyses, areas of tau accumulation and volume loss that correlated with each neurological symptom were binarized as ROIs. Using these ROIs, florzolotau (18F) SUVRs and brain volumes were calculated for each PSP case. Path analysis was used to estimate the relationships among tau accumulations (florzolotau (18F) SUVRs), structural atrophy, and scores of PSP Rating Scale subdomains, assuming a specified causal direction. Details of these analyses are provided in the supplementary flow map (Figure S1). The assessments were performed using RStudio (version 2023. 09.1+494, RStudio, PBC) and the R package lavaan[21] (version 0.6–16). We defined tau deposition as an independent variable, atrophy as a mediator, and symptomatic domain as a dependent variable and investigated direct and indirect effects. The model fit was evaluated using the normed fit index, comparative fit index, and root mean square error approximation in all patients with PSP. Akaike's information criterion was used to determine a better model. In addition, participants were divided into three groups according to the disease duration, consisting of early (1 year), intermediate (2 years), and advanced (≥3 years) chronological stages. Path analysis was then applied to individual stages to assess time-course changes in the contribution of the independent variable and mediator to the outcome measure.

Statistical Analysis

Independent sample t- and χ^2 tests were conducted to compare baseline demographics and clinical characteristics. All these statistical tests were two-tailed, with $P < 0.05$ indicating statistical significance. Values were all reported as means with standard deviations. Statistical analyses for demographics were performed using IBM SPSS Statistics for Mac, version 28.0.1.1 (IBM Corp., Armonk, NY, USA) and Prism 9 for Mac, version 9.5.0 (GraphPad Software, Boston, USA).

Data Sharing

Requests for data supporting our findings should be directed to the corresponding author, Hironobu Endo (endo.hironobu@qst.go.jp).

Results

Patient Backgrounds

The demographic profiles of the PSP patients and HCs are provided in Table 1.

Exhaustive Voxel-based Assessments

Comparisons between PSP and HC groups

The retention of florzolotau (18F) was enhanced in the subcortical structures, such as the midbrain, basal ganglia, and frontal regions of PSP cases relative to HCs (red and yellow in Figure 1), in line with the distribution of tau pathologies in this illness. These patients also presented reduced volumes of characteristic brain areas, including the midbrain, basal ganglia, thalamus, and cerebellar hemispheres, compared with HCs (green and yellow in Figure 1). There were notable spatial overlaps between tau depositions and atrophy in the midbrain and basal ganglia (yellow in Figure 1).

Topology of tau accumulation and volume loss associated with neurological symptoms

(A) Total PSP Rating Scale scores

Intensified florzolotau (18F) signals and volume declines in subcortical locations, including the midbrain, subthalamic nucleus, and globus pallidus, were correlated with increases of total PSP Rating Scale scores (upper left panels in Figure 2). Hence, there were marked overlaps between the topologies of tau depositions and atrophy related to these symptomatic scores.

(B) Ocular motor symptom domain

Tau accumulations and reduced volumes in subcortical structures, including the midbrain tegmentum and globus pallidus, were correlated with elevated PSP Rating Scale subscores in the ocular motor domain (upper right panels in Figure 2). The voxels highlighted in PET and MRI assays presented remarkable spatial overlaps.

(C) Gait and midline symptom domain

Tau depositions and volume reductions in subcortical structures, including the subthalamic nucleus and surrounding thalamic regions, alongside the globus pallidus, showed correlations with increases of PSP Rating Scale subscores in the gait and midline domain (lower left panels in Figure 2). The voxels highlighted in tau PET and MRI assays displayed notable overlaps in these locations. In addition, we observed associations of tau accumulations in the occipital cortex and volume loss in the occipital cortex and precuneus with this symptomatic domain. The neocortical voxels highlighted by tau PET and MRI showed little spatial overlaps.

(D) Limb motor symptom domain

Tau depositions and atrophy in the neocortical structures were closely associated with PSP Rating Scale subscores in the limb motor domain (lower right panels in Figure 2). There were no overlaps between distributions of augmented tau signals, which were localized to the primary to supplemental motor cortices, and volume declines, which were prominent in the angular gyrus.

The total areas of tau accumulation and volume loss associated with neurological symptoms (A)-(D) are shown as renders in Figs. S2 and S3.

(E) Other rating categories

We found no brain areas exhibiting correlations of tau accumulations or atrophy with PSP Rating Scale subscores in the history, mentation, and bulbar categories (data not shown).

Path Analysis Exploration of Causal Directions

Areas of tau accumulation and volume loss correlated with each neurological symptom were binarized as ROIs. Using these ROIs, florzolotau (18F) SUVRs and brain volumes were calculated for each PSP case.

Path analysis was performed using ROI values and PSP Rating Scale subscores in the individual domain to examine the dependencies of the key symptoms on tau depositions and volume declines and the dependencies of the volume declines on tau depositions in characteristic brain regions with possible causality directions, which was subjected to age and sex linear corrections (Figure S4).

We observed strong dependencies of symptoms in the ocular motor and gait and midline domains on the volume loss, with smaller direct effects of tau accumulations on the volume loss and symptoms (Fig. S4a, b). Limb motor manifestations were also greatly dependent on the volume loss, which markedly depended on tau depositions (Figure S4c). Considering that the disease durations were 3 years or longer in a large proportion of the PSP cases (30/53), these findings primarily reflected causality links at rather late stages.

We therefore analyzed the patients divided into early, intermediate, and advanced groups based on the disease duration to assess transitions of the associations along the time course (Figs. 3 and S5). In the path analysis of the ocular motor domain, a causality direction from tau pathologies to atrophy was the most pronounced at early and intermediate phases in contrast to the predominance of the direction from atrophy to

symptoms at the advanced stage. In the analysis of the gait and midline domain, the dependency of volume declines on tau accumulations was prominent at the early stage, similar to the ocular motor domain, whereas the causal connection atrophy to symptoms already became predominant at the intermediate stage. In the analysis of the limb motor domain, the direct dependency direction from tau depositions to symptoms dominated at the early stage, which was replaced by the pathway from tau depositions to remote atrophy and then the pathway from atrophy to symptoms along the disease time course.

The stage-wise path analysis was also carried out with partial volume corrections for the PET measures, but the findings did not overtly differ from those without corrections (Fig. S6).

Discussion

In this study, we generated high-contrast maps delineating tau pathology and regional volume loss in the brains of PSP cases, representing the largest cohort analyzed to date. Our analyses revealed, for the first time, the spatial distribution of tau deposits and brain atrophy in relation to core symptomatic domains captured by the PSP Rating Scale. Integrating these findings with path analyses of clinical and neuroimaging data, we demonstrate that subcortical tau accumulation leads to neuronal loss and localized tissue atrophy, directly contributing to symptom expression. In contrast, neocortical tau deposits appear to induce network dysfunction as well, resulting in secondary neuronal degeneration in anatomically distant regions. These distinct mechanisms of tau-induced neurotoxicity underpin the differential patterns of subcortical and neocortical pathology in PSP.

Comparisons between the PSP and control groups revealed a spatial concordance of tau pathology and volume reduction in the midbrain, basal ganglia, subthalamic nucleus, and adjacent thalamic regions of PSP brains (Fig. 1). In contrast, despite the presence of tau aggregates in the primary and supplementary motor cortices, significant neocortical atrophy ($p < 0.05$, FWE) was not observed (Fig. 1). These findings suggest that morphometric alterations in PSP are predominantly subcortical, while neocortical neuronal loss may be more heterogeneous across individuals. Indeed, reduced volumes in posterior cortical areas were evident in patients exhibiting severe "gait and midline" and "limb motor" symptoms (Fig. 2C, D).

Although prior neuropathological studies have reported interneuron loss in the primary motor cortex alongside extensive glial and neuronal tau inclusions[22], the relative preservation of large pyramidal neurons may mitigate detectable atrophy in this region. This notion aligns with a previous report documenting sparing of the motor cortex volume in PSP-Richardson type [14]. Conversely, degeneration of cortico-cortical projection neurons was identified in the pre-supplementary motor area[22], and tau-induced axonal pathology may also disrupt intercortical pathways originating from the primary motor cortex. These degenerative processes could impair the delivery of trophic support from axonal terminals to downstream regions, such as the angular gyrus, ultimately leading to transneuronal degeneration and atrophy in areas remote from dense tau accumulations.

We observed substantial spatial overlap between regions of tau accumulation and brain atrophy, which were closely associated with total PSP Rating Scale scores and subscores in the "ocular motor" and "gait and midline" domains. These voxel-wise correlational analyses primarily identified subcortical structures. Notably, impairments

in the "ocular motor" domain showed strong correlations with both tau pathology and volume loss in the midbrain. Upgazed palsy is a well-established ocular motor sign of PSP, and prior lesion studies have implicated the rostral interstitial nucleus of the medial longitudinal fasciculus (riMLF) in the midbrain as a critical site underlying this dysfunction [23]. The present tau and atrophy maps revealed the involvement of medial midbrain regions encompassing the medial longitudinal fasciculus (highlighted in yellow in Fig. 2B and the upper left panel of Fig. 3), supporting the presence of local neurodegeneration driven by tau pathology in key structures responsible for generating fast vertical eye movements.

Importantly, the superior colliculus (SC) plays a modulatory role in the activity of riMLF, which is critical for controlling eye movements[24]. Disruptions in the sequential pathways linking the globus pallidus to the SC—via the subthalamic nucleus and substantia nigra pars reticulata (SNr)—have been implicated in the pathophysiology of ocular motor dysfunction [25, 26]. Consistently, our analysis identified the globus pallidus, subthalamic nucleus, and SNr as regions showing significant associations between tau deposition, structural atrophy, and impairment in the "ocular motor" domain (highlighted in yellow in Fig. 2B). Furthermore, path analysis (upper panel in Fig. 3) suggests a sequential relationship among tau accumulation, atrophy, and symptom progression, unfolding over several years. This timeline aligns with clinical observations that gaze abnormalities typically become prominent during the middle to late stages of PSP, particularly in non-classical phenotypes[27].

As mentioned above, regions exhibiting tau deposition and volume loss associated with the "gait and midline" domain substantially overlapped with subcortical areas implicated in "ocular motor" deficits, whereas the brainstem appeared to be less

involved. The subcortical locomotive network includes the striatum, globus pallidus, subthalamic nucleus, mesencephalic locomotor region, and pontine and medullary reticular formations[28, 29]. Among these, the subthalamic nucleus and basal ganglia (highlighted in yellow in Fig. 2B and the middle-left panel of Fig. 3) were prominently identified in our correlational analysis. These structures are implicated from the early stages of PSP, including phenotypes with spatially restricted tau accumulation such as PSP-parkinsonism and PSP-pure akinesia with gait freezing[30], and are accordingly more consistently involved in locomotive impairment than the brainstem.

Gait disturbances, particularly balance difficulties and falls, frequently represent the earliest clinical manifestations of PSP, reinforcing the association between these subcortical structures and the "gait and midline" subscores. Correspondingly, path analysis (middle panels of Fig. 3) suggested a causal pathway from early-stage tau accumulation to impairments in this functional domain within one year of symptom onset.

In addition, tau deposition and atrophy in distinct neocortical regions were also correlated with "gait and midline" symptoms, indicating that tau-associated neuronal loss in remote areas may contribute to these deficits. Tau accumulation in the lateral occipital cortex, including the secondary visual cortex (V_2), may disrupt visual processing relevant to locomotion [31], while atrophy in the precuneus may compromise sensory integration required for spatiotemporal control of motor behavior[31, 32]. Given the known functional connectivity between V_2 and the dorsal precuneus[33], tau deposition in V_2 may adversely affect neuronal viability in the precuneus via axonal projections. Alternatively, tau pathology in the thalamus may impact the precuneus through their strong structural and functional connectivity[34].

Unlike the "ocular motor" and "gait and midline" domains, subscores of the "limb motor" domain primarily correlated with pathological changes in the neocortex. Tau deposition and atrophy in distinct cortical regions were associated with this domain (Fig. 2D). Notably, the primary motor cortex and supplementary motor area, along with adjacent subcortical white matter, showed left-dominant associations between tau accumulation and limb motor symptoms. This finding aligns with prior evidence that neurofunctional impairments in these regions, particularly within the left hemisphere, can disrupt motor planning for limb movements, often manifesting as limb apraxia in PSP[35-37].

We also observed correlations between volume loss in the angular gyrus and limb motor deficits, consistent with the known involvement of this parietal region in limb apraxia[38]. Tau accumulation in the primary and supplementary motor cortices may secondarily affect neurons in downstream projection sites. In support of this, the superior longitudinal fasciculus, which connects the primary motor cortex and angular gyrus [39], may serve as a conduit for trans neuronal degeneration contributing to volume loss in this region. Moreover, the motor cortex and parietal lobe, including the angular gyrus, are conceived to form a sensory-motor integration loop, and dysfunction within this loop may contribute to dystonia, a key feature of the "limb motor" domain[40].

Although the domain also includes parkinsonian features such as limb rigidity and tremor, subcortical regions typically associated with the extrapyramidal system were not prominently implicated in the present analysis. This may reflect the item composition of the domain, which emphasizes functions, such as dystonia and fine motor tasks (e.g., finger and toe tapping), that are more reliant on cortical motor circuits [40 41].

Our path analysis (lower panel of Fig. 3) suggested a directional relationship from early-stage tau deposition to limb motor impairments by less than one year of onset, indicating that tau-induced dysfunction within cortical motor areas may precede significant neuronal loss. As the disease progresses, atrophy in distant projection sites likely emerges, contributing to the focal and network-level motor deficits observed in advanced PSP.

Despite the current findings highlighting localized tau pathologies and neuronal loss associated with specific symptom domains in PSP, the large-scale impact of tau deposition on neural network degeneration, particularly remote atrophy and functional impairments, remains to be elucidated. Future investigations employing tract-specific analyses, such as diffusion tensor imaging, will be essential to address this gap. In this study, we did not account for PSP subtypes when examining pathology-symptom relationships, as the domain-based structure of the PSP Rating Scale is independent of clinical phenotype classifications. Consequently, the distinct tau topographies associated with PSP-Richardson syndrome versus other variants such as PSP-parkinsonism, and their links to symptomatic heterogeneity, are yet to be clarified. Furthermore, while our path analysis suggested temporal sequences linking tau accumulation and regional atrophy to specific symptom domains, these observations require validation in longitudinal neuroimaging studies.

In conclusion, by leveraging high-contrast PET imaging of four-repeat tau assemblies, the present study delineates the spatiotemporal profiles of neurodegenerative tau pathologies underlying the emergence and progression of specific symptom domains in PSP. This approach holds promises for predicting clinical

outcomes across the natural course of the disease and in the context of anti-tau therapeutic interventions.

Acknowledgment

This study was supported by AMED under grants JP19dm0207072, JPMJMS2024, wm0625001; MEXT KAKENHI grant JP21K15705; Biogen Idec Inc.; and APRINOIA Therapeutics. We thank all patients and their caregivers, as well as volunteers, for their participation in this study; clinical research coordinators; PET and MRI operators; radiochemists; and research ethics advisers at Quantum Science and Technology (QST) for their assistance with the current projects. We acknowledge the support of M. Kubota, Y. Yamamoto, and S. Kitamura at QST. We thank APRINOIA Therapeutics for kindly sharing the precursor of florzolotau (18F). We acknowledge the support of S. Hirano at the Department of Neurology, Chiba University on patient recruitment; T. Hatano, T. Tsunemi, N. Nishikawa, K. Nishioka (currently working at The Juntendo Tokyo Koto Geriatric Medical Center**),** Y. Yamashita, Y. Motoi, and S. Saiki (currently working at the University of Tsukuba) at the Department of Neurology, Juntendo University School of Medicine; I. Aiba at the Department of Neurology, National Hospital Organization Higashinagoya National Hospital; Y. Nakano (currently working at The Feinstein Institute for Medical Research) at the Department of Neurology, Chibaken Saiseikai Narashino Hospital; T. Yuasa at the Department of Neurology, Kamagaya General Hospital; H. Imai at the Tokyo Rinkai Hospital; Y. Nishida and Y. Yagi at the Department of Neurology, Tokyo Medical and Dental University; S. Furukawa at the Narita Red Cross Hospital; M. Seki at the Department of Neurology, Keio University School of Medicine; and T. Takeda and I. Isose at the

Department of Neurology, Chiba-East Hospital.

Author Contributions

Listed in supplement.

Potential Conflicts of Interest

M.-R.Z., H. Shimada, and M.H. hold patents on compounds related to this report.

Data Availability

The data supporting our study findings are available from the corresponding author upon reasonable request.

References

1. Yoshida M. Astrocytic inclusions in progressive supranuclear palsy and corticobasal degeneration. Neuropathology. 2014 Dec;34(6):555-70.

2. Steele JC, Richardson JC, Olszewski J. Progressive Supranuclear Palsy. A Heterogeneous Degeneration Involving the Brain Stem, Basal Ganglia and Cerebellum with Vertical Gaze and Pseudobulbar Palsy, Nuchal Dystonia and Dementia. Arch Neurol. 1964 Apr;10:333-59.

3. Williams DR, Holton JL, Strand C, et al. Pathological tau burden and distribution distinguishes progressive supranuclear palsy-parkinsonism from Richardson's syndrome. Brain. 2007 Jun;130(Pt 6):1566-76.

4. Dickson DW, Ahmed Z, Algom AA, Tsuboi Y, Josephs KA. Neuropathology of variants of progressive supranuclear palsy. Curr Opin Neurol. 2010 Aug;23(4):394-400.

5. Cairns NJ, Ghoshal N. FUS: A new actor on the frontotemporal lobar degeneration stage. Neurology. 2010 Feb 2;74(5):354-6.

6. Kato N, Arai K, Hattori T. Study of the rostral midbrain atrophy in progressive supranuclear palsy. J Neurol Sci. 2003 Jun 15;210(1-2):57-60.

7. Dutt S, Binney RJ, Heuer HW, et al. Progression of brain atrophy in PSP and CBS over 6 months and 1 year. Neurology. 2016 Nov 8;87(19):2016-25.

8. Kimura T, Ono M, Seki C, et al. A quantitative in vivo imaging platform for tracking pathological tau depositions and resultant neuronal death in a mouse model. Eur J Nucl Med Mol Imaging. 2022 Nov;49(13):4298-311.

9. Priyanka, Qamar SH, Visanji NP. Toward an animal model of Progressive Supranuclear Palsy. Front Neurosci. 2024;18:1433465.

10. Kovacs GG, Lukic MJ, Irwin DJ, et al. Distribution patterns of tau pathology in progressive supranuclear palsy. Acta Neuropathol. 2020 Aug;140(2):99-119.

11. Tagai K, Ono M, Kubota M, et al. High-Contrast In Vivo Imaging of Tau Pathologies in Alzheimer's and Non-Alzheimer's Disease Tauopathies. Neuron. 2021 Jan 6;109(1):42-58 e8.

12. Endo H, Tagai K, Ono M, et al. A Machine Learning-Based Approach to Discrimination of Tauopathies Using [^{18}F]PM-PBB3 PET Images. Mov Disord. 2022 Nov;37(11):2236-46.

13. Li L, Liu FT, Li M, et al. Clinical Utility of (18) F-APN-1607 Tau PET Imaging in Patients with Progressive Supranuclear Palsy. Mov Disord. 2021 Oct;36(10):2314-23.

14. Whitwell JL, Tosakulwong N, Botha H, et al. Brain volume and flortaucipir analysis of progressive supranuclear palsy clinical variants. Neuroimage Clin. 2020;25:102152.

15. Marquie M, Normandin MD, Meltzer AC, et al. Pathological correlations of [F-

18]-AV-1451 imaging in non-alzheimer tauopathies. Ann Neurol. 2017 Jan;81(1):117-28.

16. Malpetti M, Kaalund SS, Tsvetanov KA, et al. In Vivo (18)F-Flortaucipir PET Does Not Accurately Support the Staging of Progressive Supranuclear Palsy. J Nucl Med. 2022 Jul;63(7):1052-7.

17. Hoglinger GU, Respondek G, Stamelou M, et al. Clinical diagnosis of progressive supranuclear palsy: The movement disorder society criteria. Mov Disord. 2017 Jun;32(6):853-64.

18. Yamane T, Ishii K, Sakata M, et al. Inter-rater variability of visual interpretation and comparison with quantitative evaluation of (11)C-PiB PET amyloid images of the Japanese Alzheimer's Disease Neuroimaging Initiative (J-ADNI) multicenter study. Eur J Nucl Med Mol Imaging. 2017 May;44(5):850-7.

19. Golbe LI, Ohman-Strickland PA. A clinical rating scale for progressive supranuclear palsy. Brain. 2007 Jun;130(Pt 6):1552-65.

20. Tagai K, Ikoma Y, Endo H, et al. An optimized reference tissue method for quantification of tau protein depositions in diverse neurodegenerative disorders by PET with (18)F-PM-PBB3 ((18)F-APN-1607). Neuroimage. 2022 Dec 1;264:119763.

21. Rosseel Y. lavaan: An R Package for Structural Equation Modeling. J Stat Softw. 2012 May;48(2):1-36.

22. Halliday GM, Macdonald V, Henderson JM. A comparison of degeneration in motor thalamus and cortex between progressive supranuclear palsy and Parkinson's disease. Brain. 2005 Oct;128(Pt 10):2272-80.

23. Buttner-Ennever JA, Buttner U, Cohen B, Baumgartner G. Vertical glaze paralysis and the rostral interstitial nucleus of the medial longitudinal fasciculus. Brain. 1982 Mar;105(Pt 1):125-49.

24. Dash S, Nazari SA, Yan X, Wang H, Crawford JD. Superior Colliculus Responses to Attended, Unattended, and Remembered Saccade Targets during Smooth Pursuit Eye Movements. Front Syst Neurosci. 2016;10:34.

25. Lal V, Truong D. Eye movement abnormalities in movement disorders. Clin Park Relat Disord. 2019;1:54-63.

26. Halliday GM, Hardman CD, Cordato NJ, Hely MA, Morris JG. A role for the substantia nigra pars reticulata in the gaze palsy of progressive supranuclear palsy. Brain. 2000 Apr;123 (Pt 4):724-32.

27. Phokaewvarangkul O, Bhidayasiri R. How to spot ocular abnormalities in progressive supranuclear palsy? A practical review. Transl Neurodegener. 2019;8:20.

28. la Fougere C, Zwergal A, Rominger A, et al. Real versus imagined locomotion: a [18F]-FDG PET-fMRI comparison. Neuroimage. 2010 May 1;50(4):1589-98.

29. Hinton DC, Thiel A, Soucy JP, Bouyer L, Paquette C. Adjusting gait step-by-step: Brain activation during split-belt treadmill walking. Neuroimage. 2019 Nov 15;202:116095.

30. Williams DR, Lees AJ. Progressive supranuclear palsy: clinicopathological concepts and diagnostic challenges. Lancet Neurol. 2009 Mar;8(3):270-9.

31. Bommarito G, Putzolu M, Avanzino L, et al. Functional Correlates of Action Observation of Gait in Patients with Parkinson's Disease. Neural Plast. 2020;2020:8869201.

32. Cavanna AE, Trimble MR. The precuneus: a review of its functional anatomy and behavioural correlates. Brain. 2006 Mar;129(Pt 3):564-83.

33. Zhang S, Li CS. Functional connectivity mapping of the human precuneus by resting state fMRI. Neuroimage. 2012 Feb 15;59(4):3548-62.

34. Cunningham SI, Tomasi D, Volkow ND. Structural and functional connectivity of the precuneus and thalamus to the default mode network. Hum Brain Mapp. 2017 Feb;38(2):938-56.

35. Perlova K, Schmidt CC, Fink GR, Weiss PH. The role of the left primary motor cortex in apraxia. Neurol Res Pract. 2025 Jan 9;7(1):2.

36. Watson RT, Fleet WS, Gonzalez-Rothi L, Heilman KM. Apraxia and the supplementary motor area. Arch Neurol. 1986 Aug;43(8):787-92.

37. Soliveri P, Piacentini S, Girotti F. Limb apraxia in corticobasal degeneration and progressive supranuclear palsy. Neurology. 2005 Feb 8;64(3):448-53.

38. Metaireau M, Osiurak F, Seye A, Lesourd M. The neural correlates of limb apraxia: An anatomical likelihood estimation meta-analysis of lesion-symptom mapping studies in brain-damaged patients. Neurosci Biobehav Rev. 2024 Jul;162:105720.

39. Wang X, Pathak S, Stefaneanu L, Yeh FC, Li S, Fernandez-Miranda JC. Subcomponents and connectivity of the superior longitudinal fasciculus in the human brain. Brain Struct Funct. 2016 May;221(4):2075-92.

40. Perruchoud D, Murray MM, Lefebvre J, Ionta S. Focal dystonia and the Sensory-Motor Integrative Loop for Enacting (SMILE). Front Hum Neurosci. 2014;8:458.

41. Witt ST, Laird AR, Meyerand ME. Functional neuroimaging correlates of finger-tapping task variations: an ALE meta-analysis. Neuroimage. 2008 Aug 1;42(1):343-56.

Figure Legends

Figure 1: Topologies of tau accumulation and atrophy in the brains of PSP patients relative to controls

Voxel-based analysis showed an elevated tau PET tracer retention (red) primarily in the basal ganglia and frontal lobes, atrophy (green) in the basal ganglia, thalamus, and cerebellar hemispheres, and their spatial overlaps (yellow) in the midbrain and basal ganglia of the PSP group relative to HCs ($P < 0.05$, family-wise error corrected per cluster). Cluster size thresholds (k) are 121 voxels for tau accumulation and 79 voxels for atrophy. Areas are highlighted in the standard anatomical space of the brain.

Figure 2: Distributions of tau accumulation (red), atrophy (green), and their overlaps (yellow) correlating with neurological symptoms.

(A) Total PSP Rating Scale scores correlated with tau accumulation ($P < 0.01$) and atrophy ($P < 0.001$) commonly in the subthalamic nucleus and globus pallidus. Cluster size thresholds (k) are 1423 voxels for tau accumulation and 274 voxels for atrophy. (B) "Ocular motor" subscores correlated with tau accumulation ($P < 0.01$) and atrophy ($P < 0.001$) commonly in the midbrain tegmentum and globus pallidus. Cluster size thresholds (k) are 1425 voxels for tau accumulation and 279 voxels for atrophy. (C) "Gait and midline" subscores correlated with tau accumulation ($P < 0.01$) in the globus pallidus to thalamic area and occipital cortex and atrophy ($P < 0.001$) in the globus pallidus to the thalamic area, occipital cortex, and precuneus. Cluster size thresholds (k) are 1420 voxels for tau accumulation and 266 voxels for atrophy. (D) "Limb motor" subscores correlated with tau accumulation ($P < 0.01$) in the precentral to supplementary motor cortex and atrophy ($P < 0.001$) in the angular gyrus. Cluster size

thresholds (k) are 1390 voxels for tau accumulation and 274 voxels for atrophy. Areas are highlighted in the standard anatomical space of the brain.

Figure 3: Path analysis revealed temporal transitions in the causal relationships among tau deposition, brain atrophy, and clinical symptoms across disease progression

Causality directions were examined in the groups classified by the disease duration (early, 1 year; intermediate, 2 years; advanced, ≥3 years). In the "ocular motor" domain, tau pathology primarily drove atrophy in the early and intermediate stages, while atrophy more strongly predicted symptoms at the advanced stage. In the "gait and midline" domain, tau-driven atrophy was evident early, but atrophy-to-symptom causality became dominant by the intermediate stage. In the "limb motor" domain, early symptoms were directly linked to tau deposition, with later stages showing a sequential pathway from tau to atrophy and then to symptoms.

Table 1: Demographic characteristics.

	PSP (n = 53)	HC (n = 45)	P-value
Women, n (%)	19 (35.8)	19 (42.2)	0.519
Age, mean ± SD (years)	72.2 ± 8.1	62.9 ± 13.5	< 0.001
Disease duration, mean ± SD (years)	3.9 ± 3.4	N/A	N/A
PSP Rating Scale total (point), mean ± SD/(maximum)	35.6 ± 15.5/100	0.8 ± 1.6/100	< 0.001
History (point), mean ± SD/(maximum)	8.4 ± 4.8/24	0.1 ± 0.6/24	< 0.001
Mentation (point), mean ± SD/(maximum)	2.6 ± 2.9/16	0.0 ± 0.0/16	< 0.001
Bulbar (point), mean ± SD/(maximum)	2.8 ± 2/8	0.0 ± 0.0/8	< 0.001
Ocular motor (point), mean ± SD/(maximum)	7.3 ± 3.8/16	0.2 ± 0.5/16	< 0.001
Limb motor (point), mean ± SD/(maximum)	4.5 ± 2/16	0.4 ± 0.9/16	< 0.001
Gait and midline (point), mean ± SD/(maximum)	10.3 ± 5/20	0.1 ± 0.3/20	< 0.001

Data are expressed as the number (%), mean ± SD for normally distributed variables.

HC, healthy control; PSP, progressive supranuclear palsy

Table 2: Demographic characteristics in three disease duration subgroups.

	Disease duration			P-value
	1 year (n = 9)	2 years (n = 14)	≥3 years (n = 30)	
Women, n (%)	2 (22.2)	6 (42.9)	11 (36.7)	0.596
Age, mean±SD (years)	68.0 ± 8.9	74.9 ± 8.0	72.2 ± 7.2	0.997
Disease duration, mean ± SD (years)	1.0 ± 0.0	2.0 ± 0.0$^{\#\#\#\#}$	5.6 ± 3.6****	< 0.001
PSP Rating Scale total (point), mean ± SD/(maximum)	24.0 ± 11.0/100	28.5 ±13.7$^{\#}$/100	42.4 ± 14.0**/100	< 0.001
History (point), mean ± SD/(maximum)	5.4 ± 3.9/24	5.8 ± 4.0$^{\#}$/24	10.5 ± 4.4*/24	0.003
Mentation (point), mean ± SD/(maximum)	1.4 ± 1.4/16	2.4 ± 2.8/16	2.9 ± 3.1/16	0.482
Bulbar (point), mean ± SD/(maximum)	1.4 ± 1.4/8	1.6 ± 0.9$^{\#\#}$/8	3.6 ± 2.0*/8	0.001
Ocular motor (point), mean ± SD/(maximum)	5.7 ± 3.7/16	6.3 ± 3.1/16	8.1 ± 4.0/16	0.161
Limb motor (point), mean ± SD/(maximum)	4.0 ± 1.7/16	4.4 ± 1.9/16	4.6 ± 2.1/16	0.747
Gait and midline (point), mean±SD/(maximum)	6.0 ± 4.4/20	8.0 ± 5.2$^{\#}$/20	12.6 ± 3.6**/20	< 0.001

Data are expressed as the number (%), mean ± SD for normally distributed variables.

****P < 0.0001, **P < 0.01, *P < 0.05 versus 1 year group post hoc Dunn's test

$^{\#\#\#\#}$P < 0.0001, $^{\#\#}$P < 0.01, $^{\#}$P < 0.05 versus 3 years or later group post hoc Dunn's test

Figure 1

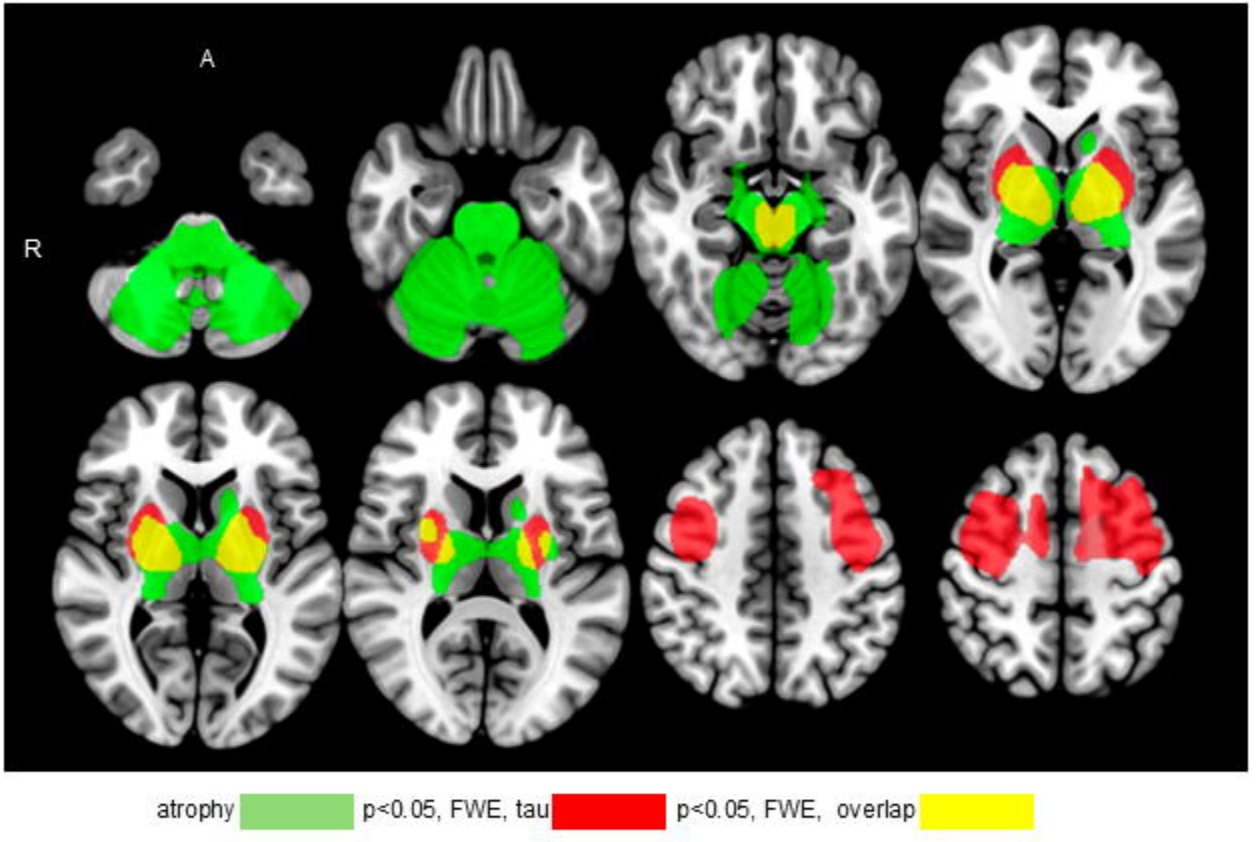

Figure 3

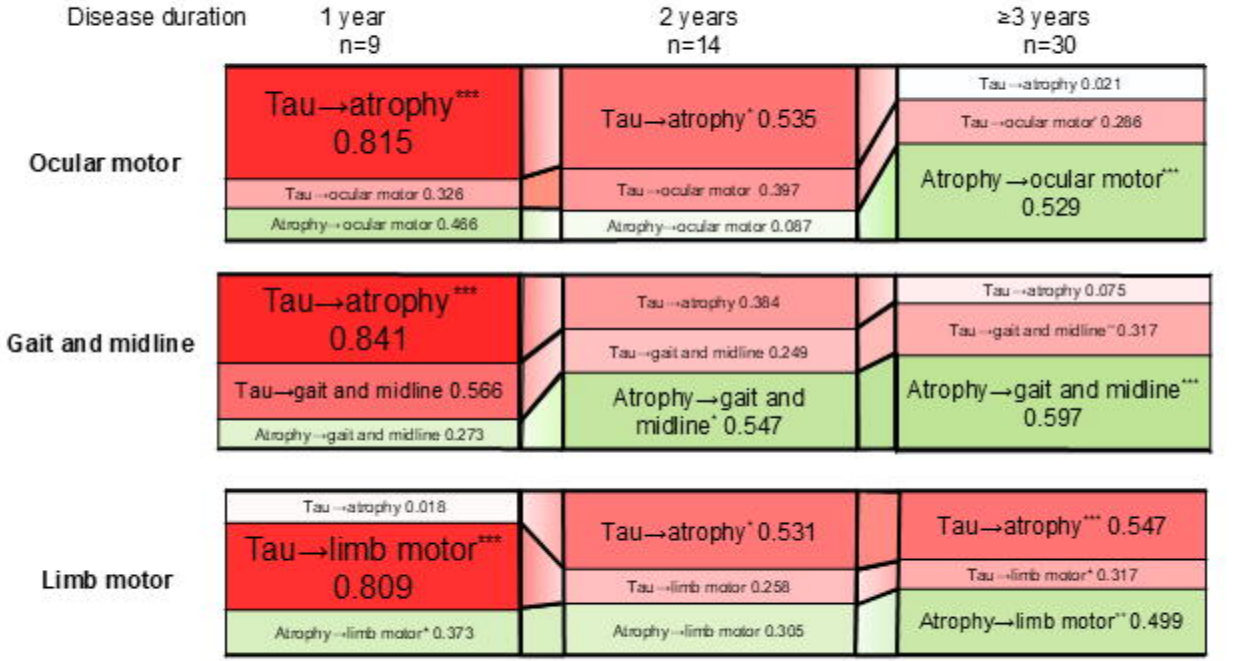

Significant at p<0.05*,p<0.01**, p<0.001***

Figure 2

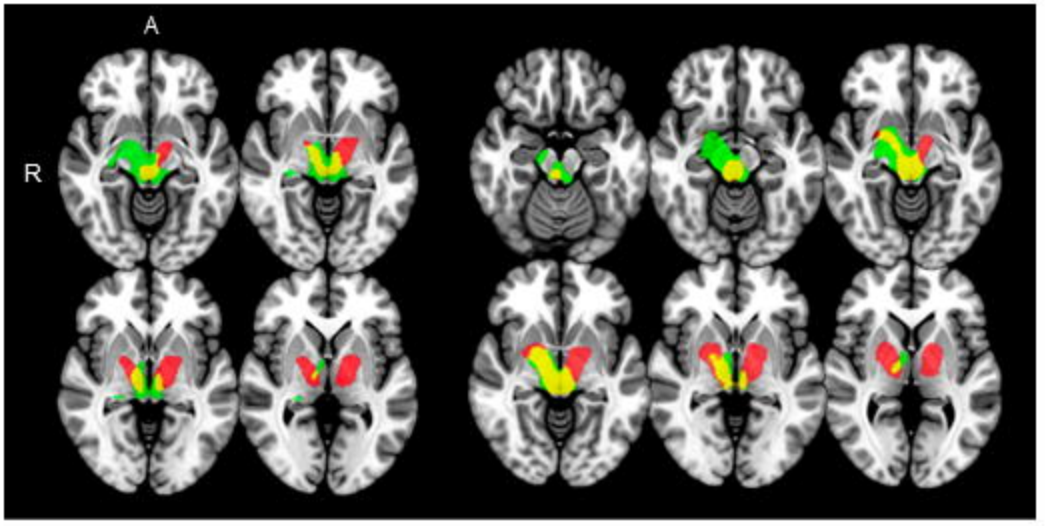

(A) Total PSP Rating Scale score (B) Ocular motor

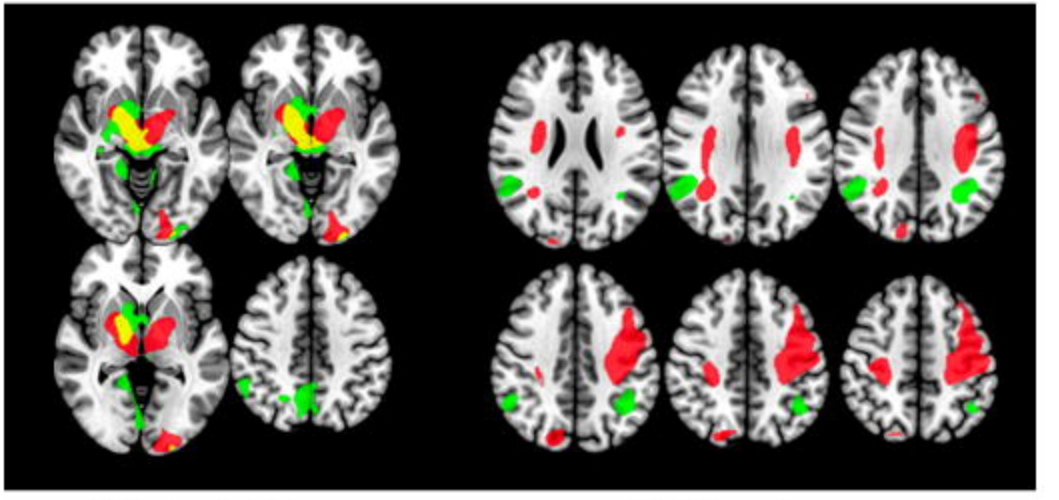

(C) Gait and midline (D) Limb motor

atrophy p<0.001, tau p<0.01, overlap